Alma Mater Studiorum Università di Bologna
Archivio istituzionale della ricerca

Bio-based and one-day compostable poly(diethylene 2,5-furanoate) for sustainable flexible food packaging: Effect of ether-oxygen atom insertion on the final properties

Bio-based and one-day compostable poly(diethylene 2,5-furanoate) for sustainable flexible food packaging: effect of ether-oxygen atom insertion on the final properties

Silvia Quattrosoldi [a,§], Giulia Guidotti [a,§], Michelina Soccio [a,c], Valentina Siracusa [b], Nadia Lotti [a,c,d]*

[a] Civil, Chemical, Environmental and Materials Engineering Department, University of Bologna, Via Terracini 28, 40131 Bologna, Italy

[b] Chemical Science Department, University of Catania, Viale A. Doria 6, 95125 Catania, Italy

[c] Interdepartmental Center for Industrial Research on Advanced Applications in Mechanical Engineering and Materials Technology, CIRI-MAM, University of Bologna, Bologna, Italy

[d] Interdepartmental Center for Agro-Food Research, CIRI-AGRO, University of Bologna, Bologna, Italy.

§ These authors contributed equally.

Abstract

In the present work, the effect of ether oxygen atom introduction in a furan ring-containing polymer has been evaluated. Solvent-free polycondensation process permitted the preparation of high molecular weight poly(diethylene 2,5-furandicarboxylate) (PDEF), by reacting the dimethyl ester of 2,5-furandicarboxylic acid with diethylene glycol. After molecular and thermal characterization, PDEF mechanical response and gas barrier properties to O_2 and CO_2, measured at different temperatures and humidity, were studied and compared with those of poly(butylene 2,5-furandicarboxylate) (PBF) and poly(pentamethylene 2,5-furanoate) (PPeF) previously determined. Both PDEF and PPeF films were amorphous, differently from PBF one. Glass transition temperature of PDEF (24 °C) is between those of PBF (39 °C) and PPeF (13 °C). As concerns mechanical response, PDEF is more flexible (elastic modulus [E] = 673 MPa) than PBF (E =1290 MPa) but stiffer than PPeF (E = 9 MPa). Moreover, PDEF is the most thermally stable (temperature of maximum degradation rate being 418 for PDEF, 407 for PBF and 414 °C for PPeF) and hydrophilic (water contact angle being 74 ° for PDEF, 90 ° for PBF and 93 ° for PPeF), with gas barrier performances very similar to those of PPeF (O_2 and CO_2 transmission rate being 0.0022 and 0.0018 for PDEF and, 0.0016 and 0.0014 cm^3 cm / m^2 d atm for PPeF). Lab scale composting experiments indicated that PDEF and PPeF were compostable, the former degrading faster, in just one day.

The results obtained are explained on the basis of the high electronegativity of ether oxygen atom with respect to the carbon one, and the consequent increase of dipoles along the macromolecule.

42

1. Introduction

Although relatively new compared to wood, glass and metals, these last used by man since the dawn of time, plastics have been used more and more and today they are practically irreplaceable. As proof of this, their production has increased from 270 million metric tons to almost 370 million metric tons from 2010 to 2020, and it is expected to further increase, rising to about 590 million metric tons by 2050.[1,2] Their global market is also expected to reach 750.1 billion of dollars by 2028.[3] Such a massive use of plastics entails a significant impact on both exploitation of non-renewable sources and on accumulation of wastes in the marine and terrestrial habitats. The environmental problems caused by human activity are one of the main themes of debate of the last Century. With the perspective of reducing the environmental issues and building a new circular economy, the employment of renewable resources for plastic production and plastic waste recycling are the most suitable solutions. For this reason, sustainable materials are attracting a continuously growing interest as potential candidates for the replacement of traditional plastics.[4,5] To date, promising results have been obtained with bioplastics, in particular with the class of bio-based polyesters.[6,9] Their bio-based nature makes them particularly interesting for applications in food packaging field, since the multilayer structure of most of the packaging currently used creates severe recycling limits.[10] Nevertheless, to be suitable for food packaging employement, a polymeric device has to satisfy strict requirements, including proper mechanical response and outstanding barrier performance.[11] Nowadays, the so-called "smart packaging" has attracted a great interest too, as a result of lifestyle changes and consumer's desire for convenient, safe and tasty food with prolonged shelf life and unaltered quality and freshness.[12,13] In these intelligent packaging systems, added materials interact with the internal environment of the package, monitoring the state of the food inside and reducing its corruption until consuming.[14-16]

Another way to reduce environmental impact, is the use of flexible packaging instead of rigid one. A LCA study commissioned by Flexible Packaging Europe in 2021 showed that flexible packages have

67 a more than 60% lower impact than their rigid counterparts.[17,18] More in detail, using flexible

68 alternatives means reducing package volumes and amount, saving space and energy during

69 transportation and minimizing wastes. As a confirmation of this, another study, carried out by the

70 Institute for Energy and Environmental Research in 2020, demonstrated that flexible packaging is

71 more effective than rigid one in preserving resources and reducing carbon footprint: if all rigid

72 packaging of non-beverage Fast Moving Consumer Goods in the European Union would be substitute

73 by flexible one, the amount of primary packaging waste could be reduced by 21 million tonnes (i.e.

74 70%) per year.[18]

75 In this framework, furan-based polyesters can be surely considered the materials of the future,[19-24]

76 since they can be used to produce a mono-material packaging, combining bio-based origin[25-31] with

77 excellent barrier properties and tunable mechanical performances, ranging from high stiffness to

78 elastomeric behavior.[32,33] More important, they can also be recycled, once the first use has been

79 accomplished.

80 When employed as food containers, plastics are often contaminated with organic matter, which

81 prevents recycling, or at least makes it very expensive,. Moreover, it must be kept in mind that an

82 efficient and sustainable plastic waste management became more complex and difficult due to

83 COVID-19.[34,35] The pandemic emergency , has determined a huge increase of food packaging plastic

84 waste due to online shopping and home delivery, accompanied by a change in mindset, according to

85 which single use plastics provides "safety". Plastic recycling increased at slower rate for fear that

86 plastic wastes might be infected, and due to the lockdown too.[36]

87 Within this scenario, which was already complex and became even more difficult due to the

88 pandemic, compostable packaging represents the best option, especially for single-use plastics.

89 Aromatic polymers, such as furan-based polyesters, are hardly attacked both by water and/or

90 microorganisms.[37-40] The development of a strategy able to enhance their modest degradation rate is

91 a really important challenge.[41,42]

92   As is well known, the strong point of plastics is the unique combination of light weight, durability,

93   low cost, ease of synthesis and the possibility to *ad hoc* modify their functional properties in view of

94   the particular application. Even though the use of additives, physical and chemical blending and

95   production of composites are very effective tools to properly tune the material performances,[24,43,44]

96   the starting point is definitely represented by a proper chemical design. Minor modifications in the

97   chemical structure of a polymer, such as the overall composition, the atomic arrangement in the

98   backbone, the length of the subunits in the repeating unit, the presence of side-groups and isomerism

99   can lead to significant variations in physical properties. [21,22,45-49] Macromolecular mobility and the

100   developed microstructure are strongly connected to the chemical structure of the polymer, thus

101   affecting features like mechanical response, thermal stability, hydrophilicity, gas barrier performance

102   and compostability.[50]

103   Considering also that 2,5-furandicarboxylic acid (FDCA) is one of 12 high value-added chemicals

104   obtained from sugars[31,51] according to the United States Department of Energy (updated in 2020),[52,53]

105   in the present work, a new 100% renewable furan-based polyester was synthesized by two-step melt

106   polycondensation reaction, following the "Green chemistry" principles. For this purpose, FDCA has

107   been coupled with diethylene glycol, recently proposed as bio-based monomer,[54] obtaining

108   poly(diethylene 2,5-furanoate) (PDEF). It is worth noting that the starting monomers, FDCA and

109   diethylene glycol, can be derived from second and third generation cellulosic feedstocks (non-food

110   crops, waste materials and algae), thus avoiding the exploitation of food and animal feed as well as

111   of land destined for food production.[55] As one can see from the PDEF chemical formula (**Scheme**

112   **1A**), an ether-oxygen atom is contained in its repeating unit. As previously evidenced for other

113   polymeric systems,[56-63] the presence of -C-O-C- moiety in the polymer backbone has several effects,

114   such as an increase in crystallinity degree decrease and wettability. These factors can potentially

115   favour the water/polymer affinity and, consequently, the hydrolytic and bacterial attack of the

116   macromolecule backbone. From the chemical structure point of view, PDEF can be considered as

117   coming from the modification of the previously studied poly(butylene 2,5-furanoate) (PBF)[33,64] and

118 poly(pentamethylene 2,5-furanoate) (PPeF).[32,33] In particular, PDEF can be obtained through the

119 insertion of an O atom (centrally located) in the glycol moiety of PBF, or by substituting the central

120 methylene group of the aliphatic subunit of PPeF with the ether-oxygen (**Scheme 1A**). To the best of

121 our knowledge, PDEF was previously synthesized by Katia Loos' group using a lipase as catalyst,[65]

122 and by Haernvall et al. through direct esterification, and characterized from the molecular, thermal

123 and enzymatic degradation point of view.[66] In addition to molecular and thermal characterization, the

124 polyester reported in the present paper was also subjected to mechanical characterization and the

125 surface hydrophilicity of the compression molded film was also evaluated. Lab-scale composting

126 experiments were carried out at 58°C at 90% humidity. Barrier performances to oxygen and carbon

127 dioxide were investigated at two different temperatures (23 and 38 °C). The effect of relative humidity

128 at 23°C was also studied. All the results obtained for PDEF were compared with the previous ones

129 got on PBF and PPeF with the aim to evaluate the effect of this chemical modification on the final

130 solid-state properties. The present work is meant to enlarge the furan-based polymer knowledge and,

131 more importantly, to lay the foundations for a deep study of structure-property relationship, which is

132 fundamental for the design of new materials addressing the desired final properties.

133

134 ## 2. Materials and methods

135 **2.1 Materials**

136 Dimethyl furan-2,5-dicarboxylate (DMF) (99%), diethylene glycol (DEG) (99%), titanium

137 tetrabutoxide (TBT), and titanium isopropoxide (TIP) were reagent-grade products. All reagents were

138 bought from Sigma-Aldrich, except DMF, which was supplied by Matrix Fine Chemicals.

139 **2.2 Synthesis**

140 Poly(diethylene 2,5-furanoate) (PDEF) was synthesized through a green solvent-less two-stage

141 polycondensation process. The reagents DMF (0.031 mol, 5.71 g) and DEG (0.062 mol, 6.58 g), in a

142 molar ratio of 1:2, were charged in a 200 mL glass reactor, together with the catalysts TBT and TIP

143 (200 ppm of both). The system was continuously stirred (50 rpm) and the temperature adjusted by a

144 silicone oil bath. A condenser cooled by liquid nitrogen was coupled to the reactor. In the first step,

145 carried out at 180 °C and under nitrogen flow, the transesterification reactions took place and

146 methanol was released off. After 90% of theoretical methanol was collected (i.e. 90 minutes), the

147 pressure was progressively reduced to 0.05 mbar, while the temperature was raised up to 230 °C. In

148 the second stage, lasting 3 hours, the reaction mass viscosity increased till a constant torque value.

149 Afterwards, the polymer (6.5 g, 95% yield) was discharged from the reactor. A lightly coloured

150 rubber-like solid was obtained. PBF and PPeF were previously synthesized by the authors through

151 the same polycondensation procedure using the same catalysts.[32,33] Briefly, for PBF the glycolic

152 molar excess was 300%, the first step was carried out at 180°C for 3 hours and the second one at

153 230°C for further 3 hours. In case of PPeF, a glycolic molar excess of 500% was adopted, the first

154 step was carried out at 170°C for 3 hours while the second one at 220°C for further 2.5 hours.

155 The as-synthesized polymer was solubilized in chloroform and then precipitated in cold methanol, in

156 order to remove residual catalysts and low molecular weight by-products.

157 **2.3 Molecular characterization**

158 Polymer chemical structure was verified by [1]H-nuclear magnetic resonance spectroscopy (Varian

159 Inova 400-MHz Instrument) at room temperature using deuterated chloroform ($CDCl_3$) as solvent.

160 The solution contains also 0.03 vol% tetramethylsilane (TMS) as an internal standard. The

161 concentration of the polymeric solution was 0.5 wt %.

162 Polymer number molecular weight (M_n) and polydispersity index (Đ) were determined by a 1100

163 HPLC system (Agilent Technologies) equipped with PLgel 5 mm MiniMIX-C column, at 30 °C.

164 Chloroform was used as the eluent, 0.3 mL/min flow, and sample concentrations of about 2 mg/mL

165 were adopted. Calibration curve was obtained using polystyrene standards in the range of 800−

166 100000 g/mol.

167 **2.4 Thermal characterization**

168 Differential Scanning Calorimetry (Perkin Elmer DSC6), calibrated with indium and cyclohexane

169 standards, was used to analyse the thermal transitions by heating from -70 °C to 190 °C at 20 °C/min

170 (I scan, resolution: 0.1 seconds between points). The sample (5 mg) was then cooled to -70 °C at 100

171 °C/min, and after that another heating scan was performed (II scan, resolution: 0.1 seconds between

172 points). The glass transition temperature (T_g) and heat capacity (Δc_p) were taken as the midpoint and

173 the height, respectively, of the heat capacity step at the glass transition. Melting temperature (T_m) and

174 crystallization temperature (T_{cc}) were determined as the peak maximum/minimum of the

175 endothermic/exothermic phenomena in the I and II heating scan DSC curves, respectively. The

176 corresponding heat of fusion (ΔH_m) and heat of crystallization (ΔH_{cc}) were obtained from the total

177 area of the DSC endothermic and exothermic signals, during the I and the II heating scans,

178 respectively. For the determination of ΔH_m and ΔH_{cc} we have used a straight baseline.

179 Thermogravimetric analysis (Perkin Elmer TGA7), was employed to evaluate the thermal stability

180 by heating 5 mg of polymer from 50 to 800°C at 10°C/min under nitrogen atmosphere (gas flow: 40

181 ml/min). The maximum degradation rate temperature (T_{max}) was calculated as the minimum of

182 thermogram derivative .

183 **2.5 Film preparation**

184 Polymer films (2.5 g, 11 x 11 cm^2, 100 μm thickness) were obtained by compression molding the

185 synthesized material with a laboratory press Carver C12. The polymer was heated to 100 °C, kept

186 under 5 ton/m^2 pressure for 2 min, removed from the press and left cooled down to room temperature.

187 Then, the films were stored at room temperature for 30 days before further characterization.

188 **2.6 Water contact angle measurements**

189 Water contact angle (WCA) determination was carried out on the compression moulded films using

190 a KSV CAM101 instrument (Helsinki, Finland) at room temperature. The side profiles of deionized

191 water drops (4 μL) on the polymer surface were analyzed just after deposition. In case of PDEF, also

192 the drop shape evolution with time was considered. At least 10 tests have been performed on different

193 film areas, from which the WCA average value ± standard deviation was determined.

2.7 Mechanical characterization

195 Tensile tests were performed on rectangular specimens (5 mm x 50 mm x 100 μm) by means of an

196 Instron 5966 testing machine with a transducer-coupled 1kN load cell (stretching rate: 10 mm/min).

197 The measurements were carried out at room temperature (23 °C) and a relative humidity of 55%.

198 Elastic modulus (E) was calculated from the initial slope of the stress-strain curve. Stress at yielding

199 (σ_y) and stress (σ_b) and elongation (ε_b) at break were also determined. These results are reported as the

200 average value ± standard deviation, obtained testing six different specimens.

2.8 Barrier properties

202 Barrier capability to oxygen and carbon dioxide was evaluated by a manometric method using a

203 Permeance Testing Device, type GDP-C (Brugger Feinmechanik GmbH), according to ASTM 1434-

204 82, DIN 53 536 and ISO/DIS 15 105-1 protocol. The measurements were performed on a film surface

205 of 78.5 cm^2, under a gas stream of 100 cm^3/min, at 23 and 38 °C, and 0 and 85 % relative humidity.

206 The results have been expressed as gas transmission rate (GTR, in cm^3 cm m^{-2} d^{-1} atm^{-1}), which defines

207 the permeability to gas of the film. The measurements were made in triplicate and the result was

208 expressed as average value ± standard deviation.

2.9 Composting tests

210 Composting studies have been carried out at 58 °C in mature compost kindly supplied by

211 HerAmbiente S.p.A. Films of about 20x20 mm^2 (50 mg) were placed in a 100 mL bottle containing

212 wet compost. Specimens were withdrawn from compost in triplicate at different time intervals,

213 washed and dried over P_2O_5.

2.10 SEM investigation

215 Surface characterization was carried out by scanning electron microscopy (SEM). SEM images were

216 acquired on a desktop Phenom microscope on metal sputtered film samples glued on aluminum

217 holders with carbon tape.

3. Results and discussion

3.1 Molecular characterization

220 In **Scheme 1A,** the chemical structure of poly(diethylene 2,5-furanoate) (PDEF) is reported, together

221 with the formulas of the two homopolymers poly(butylene 2,5-furanoate) (PBF) and

222 poly(pentamethylene 2,5-furanoate) (PPeF) to which PDEF has been compared throughout the

223 present study. All the polyesters present a furan ring in the acid subunit, the difference being in the

224 glycolic moiety. In case of PBF, four methylene groups are present. PDEF has the same number of -

225 CH_2- groups, plus an ether-oxygen atom in between, this latter replaced by a methylene group in case

226 of PPeF. PDEF could be considered as derived, on one side from PBF by the insertion of a central O

227 atom in the glycol moiety and, on the other, from PPeF by the substitution of the central -CH_2- group

228 with a -O- one.

A

Poly(butylene 2,5-furanoate) (PBF)   Poly(diethylene 2,5-furaoate) (PDEF)   Poly(pentametylene 2,5-furanoate) (PPeF).

B

PBF   PDEF

229
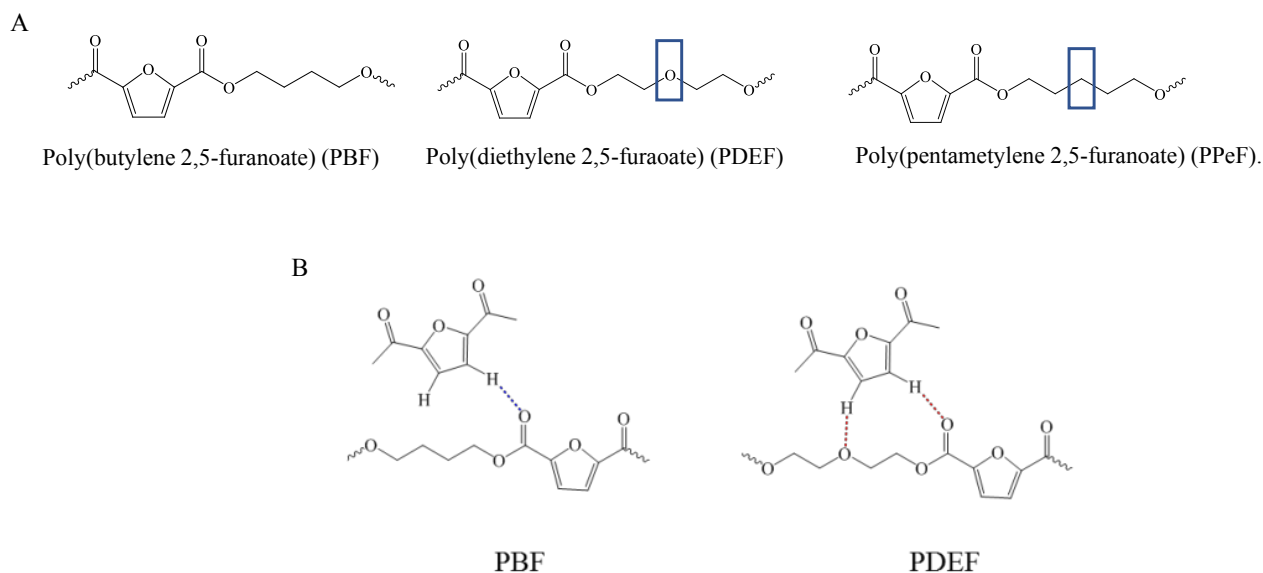
230 **Scheme 1. A)** Molecular structures of poly(diethylene 2.5-furanoate) (PDEF), poly(butylene 2,5-

231 furanoate) (PBF) and poly(pentamethylene 2,5-furanoate) (PPeF); **B)** Inter-chain hydrogen bonds in

232 PBF and PDEF matrices. For PPeF, a PBF-like behaviour was also supposed.

233

In **Fig. S1** the PDEF ^{1}H-NMR spectrum, together with the spectra of PBF and PPeF, is reported. As one can see, the expected structure for PDEF was confirmed. In details, the -CH_2- groups of the diethylene glycolic unit gave rise to two triplets at 3.82 (f) and 4.49 ppm (e), while the two d protons proper of the furan ring produced a singlet (a) located at 7.20 ppm. PBF showed the same signal at 7.34 ppm (a), then the peaks of the b and c methylene groups of the butylene subunit could be observed at 4.51 and 1.99 ppm, respectively. PPeF, beside the furan ring signal (g) at 7.20 ppm, presented three different peaks due to the methylene hydrogen atoms at 4.35 (h), 1.84 (i) and 1.57 ppm (j). The high molecular weight, obtained by means of GPC and reported in **Table 1**, confirmed the good control of the PDEF synthetic route, analogously to PBF and PPeF homopolymers.[33] The polydispersity index (Đ) resulted close to 2, as expected for a polycondensation process.

The use of traditional Titanium-based catalysts has made possible to obtain a polymer with a significantly higher molecular weight than that previously obtained by others using a lipase as catalyst.[65]

3.2 Thermal characterization

TGA analysis has been carried out to follow PDEF weight loss during heating scan under inert atmosphere (nitrogen). The corresponding thermogravimetric curve is reported in **Fig. 1A**, together with those previously obtained for PBF and PPeF, while the corresponding T_{max} values are listed in **Table 1**. The derivative curves of thermograms are reported in **Fig. S2**. It is worth noticing the high thermal stability of all the furan-based polyesters here evaluated.
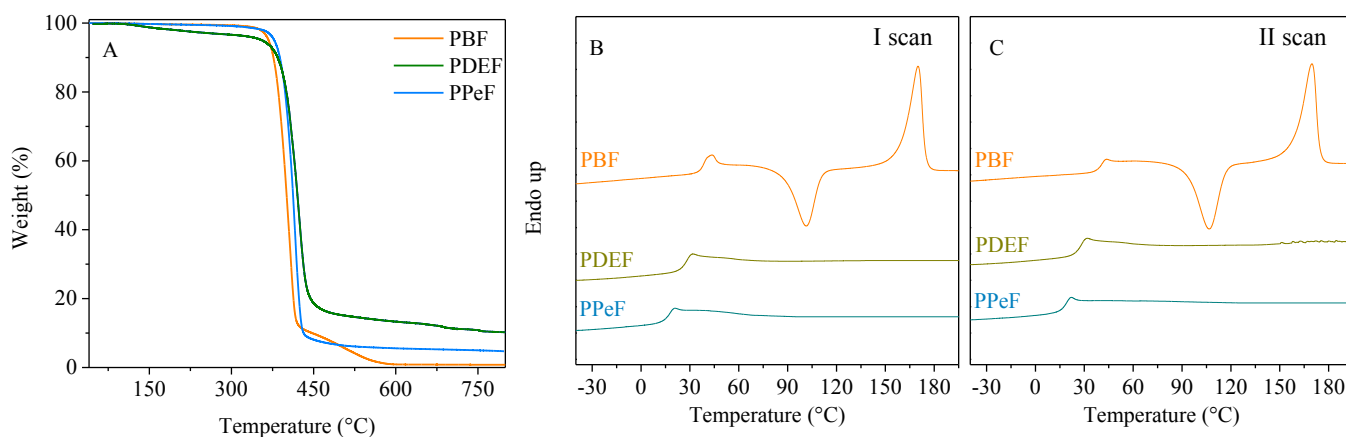
Fig. 1. A) Thermogravimetric analysis curves of PBF, PDEF and PPeF samples obtained by heating at 10°C/min under nitrogen atmosphere; **B)** DSC traces of first heating scan of the compression moulded films and **C)** second heating scan after melt quenching (20 °C/min) of PBF, PDEF, PPeF.

In agreement with previous studies,[67-69] PBF degraded at lower temperature (and comparable to the one evidenced by Kainulainen et al.[64]) compared with the other two samples, reaching the maximum degradation rate at 407°C, while PDEF had the highest stability despite an initial weight loss of 4% occurring at approximately 100°C. The presence of -O- ether linkages along the macromolecular backbone, in fact, increased the tendency of the material to absorb polar molecules as water. The evaporation of the adsorbed H_2O molecules could be likely responsible for this initial weight loss step in PDEF. The highest T_{max} value obtained for PDEF could be due to the higher energy of the C-O bond, present in the diethylene glycol moieties, less prone to random scission compared with C-C bond (358 kJ/mol vs. 346 kJ/mol, respectively[70]), proper of PBF and PPeF. Another important aspect was related to the formation of inter-chain hydrogen bonds, as shown in **Scheme 1B**. The establishment of inter-chain hydrogen bonds for furan-based polyesters, in addition to π-π interaction between the aromatic rings, has been evidenced by dielectric experiments, rheological analysis[71] and lastly proposed through simulation studies.[72] Considering the chemical structure, one can hypothesize that the presence of an ether-oxygen atom in the PDEF unit could increase the hydrogen bond density, thus improving the thermal resistance of the material, since the energy provided to polymer chains,

273 during heating, is first and preferentially used to break these physical links before breaking covalent

274 bonds. On the contrary, the lowest thermal stability of PBF among all the samples under study could

275 be ascribed to the lowest number of hydrogen bonds. The glassy state of PBF at room temperature

276 could limit the establishment of such inter-chain interactions, since at 25 °C, the PBF polymer chains

277 have lower molecular mobility than those of the rubbery PPeF sample.

278

279 Calorimetric analysis was performed in order to define the thermal transitions proper of the three

280 samples subjected to compression molding. The DSC traces and the relative data are reported in **Fig.**

281 **1** and in **Table 1**, respectively. The cooling scans between I and II heating scans reported in **Fig. S3**.

282 PBF film presented a melting peak centered at 164°C and preceded by a cold crystallization

283 endotherm located at 87°C; since $\Delta H_m > \Delta H_{cc,}$ PBF film could be considered as semicrystalline. PDEF

284 and PPeF did not present any melting peaks, showing no capability of organizing their

285 macromolecules in crystalline structure through the compression molding process, in agreement with

286 previous studies.[32,73] Just a glass transition step, respectively at 24 °C and 13 °C, was observed; in

287 both cases, the values recorded were lower than the PBF one. Looking at the chemical formulas of

288 **Scheme 1A**, one can see that PDEF and PPeF are characterized by longer glycolic subunits (PDEF:

289 4 -CH_2- and 1 -O-; PPeF: 5 -CH_2- moieties) compared with PBF (4 -CH_2- moieties). Even if the nature

290 of the atom changes, longer glycols favor macromolecular mobility, moving T_g towards lower

291 temperature.[74] $T_{g,PDEF}$ can be compared with $T_{g,PPeF}$, due to their common fully amorphous nature. As

292 one can see, $T_{g,PDEF} > T_{g,PPeF}$, the difference due to the high electronegativity of heteroatoms in the

293 glycolic unit of PDEF, favouring inter chain interactions (reduced chain mobility).

294 Despite the comparable aliphatic segment length, the highly electronegative oxygen in the glycolic

295 portion of PDEF promoted inter-chain interactions (hydrogen bonds as well as Van der Waals

296 interactions). In this way, the segmental relaxation was hampered, and thus glass transition

297 temperature increased.

298

299 **Table 1.** Molecular, thermal and mechanical characterization data of PDEF, PBF and PPeF films.

300 WCA (°) and GTR values to oxygen and carbon dioxide at 23°C, RH 0% are also collected.

		PBF	PDEF	PPeF
GPC	M_n [g/mol]	27300 ±100	21400 ±100	29600 ±100
	Đ	2.3 ±0.1	2.3 ±0.1	2.4 ±0.1
TGA	T_{MAX} [°C]	407 ±1	418 ±1	414 ±1
DSC	I SCAN	T_g [°C]	39 ±1	24 ±1	13 ±1
		ΔC_p [J/g·°C]	0.24±0.01	0.45±0.01	0.39±0.01
		T_{cc} [°C]	102 ±1	/	/
		ΔH_{cc} [J/g]	26 ±1	/	/
		T_m [°C]	170 ±1	/	/
		ΔH_m [J/g]	35 ±1	/	/
	II SCAN	T_g [°C]	39 ±1	24 ±1	13 ±1
		ΔC_p [J/g·°C]	0.28±0.01	0.47±0.01	0.43±0.01
		T_{cc} [°C]	107 ±1	/	/
		ΔH_{cc} [J/g]	30 ±1	/	/
		T_m [°C]	170 ±1	/	/
		ΔH_m [J/g]	35 ±1	/	/
Tensile test	σ_y [MPa]	11 ± 2	7 ± 1	/
	σ_b [MPa]	21 ± 3	4 ± 0.2	6 ± 1
	ε_b [%]	157 ± 10	502 ± 100	1050 ± 200
	E [MPa]	1290 ± 140	673 ± 76	9 ± 1
WCA	Ө [°]	90 ± 2	74 ± 1	93 ± 3
Barrier properties	O_2-TR [cm^3 cm / m^2 d atm]	0.10 ± 0.006	0.0022 ± 0.0002	0.0016 ± 0.0001
	CO_2-TR [cm^3 cm / m^2 d atm]	0.19 ± 0.01	0.0018 ± 0.0001	0.0014 ± 0.0001

301

302

303 The three molten samples were subjected to fast cooling and analysed during a second heating

304 measurement. As expected, PDEF and PPeF resulted again completely amorphous. As concerns PBF,

305 a major polymer fraction could be quenched in the amorphous phase thanks to the high cooling rate,

306 even though no completely amorphous sample could be obtained. As evidenced by II scan DSC trace,

307 once T_g was exceeded, PBF macromolecules were able to fold in an ordered structure ($T_{cc} = 107\ °C$;

308 $\Delta H_{cc} = 30$ J/g) which melts at higher temperature ($T_m = 170°C$; $\Delta H_m = 35$ J/g). Despite the high cooling

309 rate, ΔH_m still keeps slightly higher than ΔH_{cc}.

310 **3.3 Mechanical characterization**

311 Stress-strain measurements were conducted on PDEF films. The obtained curve is reported in **Fig. 2**,

312 while the related data are collected in **Table 1**, together with the results previously got for PBF and

313 PPeF samples. In details, PBF film showed high elastic modulus and stress at break, and quite low

314 deformation at break in line with its semicrystalline nature, together with a T_g above room

315 temperature. Differently, thanks to its amorphous nature and a T_g below room temperature, PPeF was

316 characterized by an elastic modulus reduced by two orders of magnitude, together with an outstanding

317 elongation at break (more than 1000 %). Moreover, as previously reported,[32] PPeF was able to recover

318 its initial shape thanks to a supramolecular 1-D, 2-D structure springing from inter-chain hydrogen

319 bonds established between macromolecular chains. PDEF had a mechanical behavior intermediate

320 between the one typical of a semicrystalline material, as PBF, and that of a rubbery fully amorphous

321 polymer, as PPeF. Like PBF, PDEF undergoes yielding,[75,76] a phenomenon which was not observed

322 in PPeF. The lack of crystallites in PDEF produced a reduction of E and σ_y compared to PBF. This

323 decrement was contained by the interactions among different chains, thanks to the oxygen atom of

324 the glycolic subunit, which helped keeping the elastic modulus and the strain before yielding quite

325 high. At the same time, the higher chain mobility of PDEF with respect to PBF (lower T_g), coming

326 from the introduction of O atom, allowed reaching a 500% ε_b.
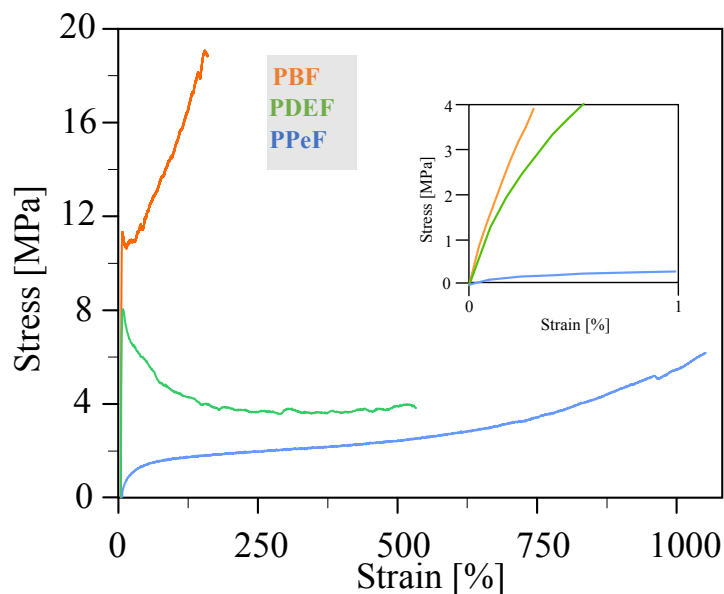
15

327

Fig. 2. Stress-strain curves of PBF, PDEF and PPeF films. In the inset the region corresponding to
low values of stress and strain is reported.

3.4 Water contact angle

In order to evaluate the surface hydrophilicity of PDEF film, the interaction between film and water
was investigated through water contact angle measurements. Particular attention was devoted to the
effect of the introduction of an oxygen atom in the polymer backbone. Again, the outcomes obtained
for PDEF film have been compared with the PBF and PPeF ones.

As it is clearly visible from **Fig. 3A** and from the data in **Table 1**, PDEF resulted the most hydrophilic
film, being the WCA_{PDEF} lower than both WCA_{PBF} and WCA_{PPeF}. These results suggest that the
introduction of ether-oxygen in the PBF repeating unit increases the polarity of the material, as
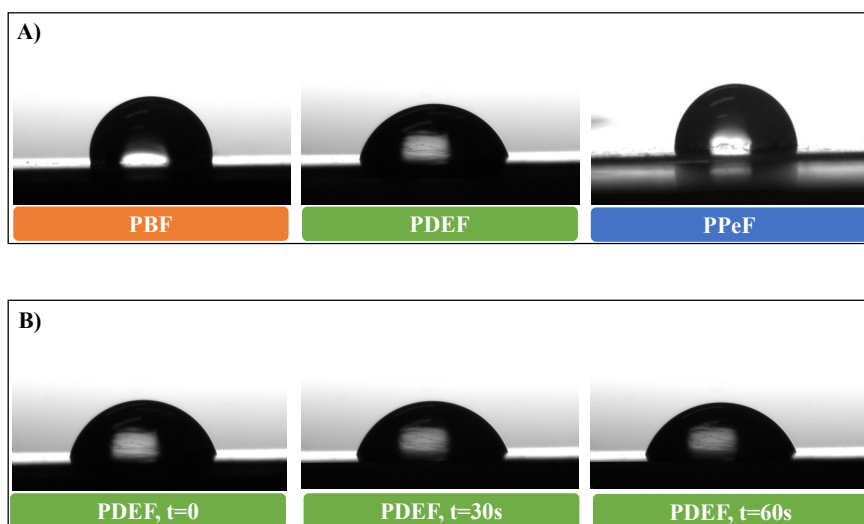already suggested by previous studies.[77]

16

Fig. 3. A) Images of water drops deposited on PBF, PDEF and PPeF films; **B)** water drop on PDEF after 0, 30 and 60 s from deposition.

The high affinity with water was in line with the TGA results obtained for PDEF. The initial weight loss observed during the thermogravimetric analysis can be ascribed to the release of the humidity absorbed from the environment. By replacing the oxygen atom of the PDEF glycolic subunit with a non-polar -CH_2- group, obtaining the PPeF chemical structure, the hydrophobic character rose again. WCA value of PPeF is similar to that of PBF, despite the greater length of the aliphatic portion (4 -CH_2- for PBF *vs.* 5 -CH_2- for PPeF).

In **Fig. 3B**, the profile change of the drop deposited on PDEF film as a function of time was reported. A clear difference in contact angle could be observed just after 30 s from the release of the water drop. A completely different behaviour was observed for PPeF and PBF, for both of which no evolution of the drop shape with time was detected. The drop shape evolution on PDEF surface is further evidence of its improved hydrophilicity with respect to PBF and PPeF.

3.5 Composting test

In order to evaluate the potential end-of-life destination of PDEF-based products, composting tests were conducted. For each sample, square shaped films were incubated in adequately prepared compost and maintained under controlled atmosphere (58°C, 90% relative humidity). Then, several

17

358 withdrawals were operated at different times (**Fig. 4**). The composting measurements were also

359 carried out on PBF and PPeF samples. As regards PBF, after 62 days in compost, no changes on the

360 film surface nor in the gravimetric weight were observed.

361
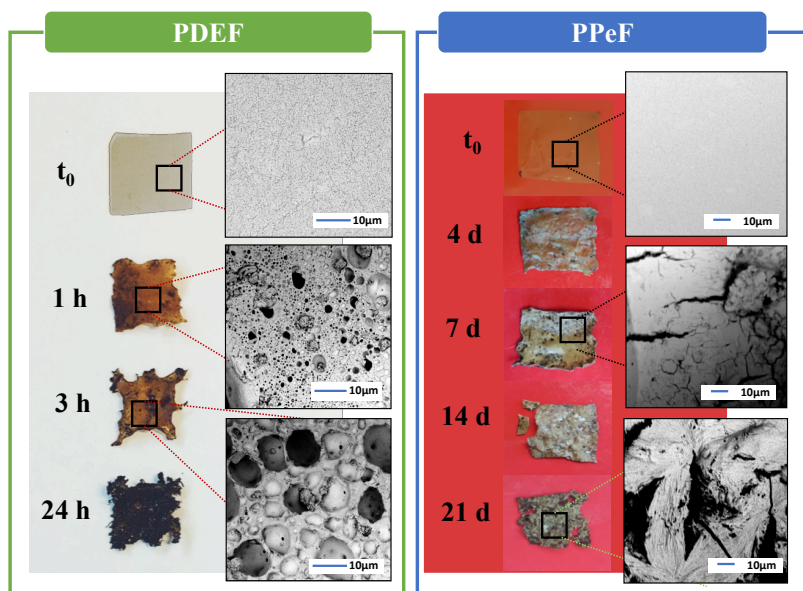
362

363 **Fig. 4.** PDEF and PPeF film images collected at different composting times: macroscopic view (left)

364 and SEM images (right).

365

366 A deeply different behaviour was observed for PDEF, which underwent degradation as soon as

367 incubated (**Fig. 4**). Just after 1 hour, the film macroscopically changed in colour and dimension, holes

368 and cracks were clearly observed with SEM. In particular, the cavities increased in size with the

369 incubation time, and after just 3 hours, the surface was almost completely covered of holes. After 24

370 hours of incubation, the film was wholly incorporated in compost. The high tendency to degrade

371 comes from the high hydrophilicity of PDEF given by the oxygen atoms inserted in the glycolic

372 subunit, and from the rubbery state of the polymer under the experimental conditions. Both these

373 features favour the diffusion of water molecules and microorganisms' attack. It is worth noting that

374 PDEF film did not undergo solubilization, as confirmed by additional experiments carried out in neat

375 water. In this case, no changes in PDEF film both at micro- and macroscopic level were observed,

376   even after months. As concerns PPeF, its degradation proceeded very fast, but at lower extent

377   compared with PDEF. Also in this case $T_{incubation} > T_{g,PPeF}$, but degradation was slowed down likely

378   because of the lower hydrophilicity. Anyway, after 4 days, macroscopical changing on the film

379   surface could be seen and, after 7 days, cracks and holes could be observed microscopically via SEM

380   analysis. In 21 days, the film was deeply compromised by degradation process both at micro- and

381   macroscopic level (**Fig. 4**). Given the compost contamination of the incubated PDEF and PPeF films,

382   it was not possible to perform weight loss measurements.

383   The huge slowing down of composting rate for PBF films has to be ascribed to its semicrystalline

384   nature and lower macromolecular mobility ($T_{g,PBF} > T_{g,PDEF}, T_{g,PPeF}$) more than to its quite high

385   hydrophobicity, being this last comparable to PPeF one ($WCA_{PBF} \approx WCA_{PPeF}$).

386   **3.6 Barrier properties**

387   Barrier properties are influenced by several factors that can have different impact on the final

388   performance. As a general trend, all factors that increase free volume among chains worsen barrier

389   properties. A pertinent example is the macromolecule flexibility, which is related to the glass

390   transition temperature. In particular, the lower the T_g the higher the number of unoccupied spaces,

391   which cause the increase of gas transmission rate (GTR). Differently, the presence of ordered phases

392   hampers the passage of gases through the film. In addition to the three-dimensional crystals, in the

393   systems containing aromatic or aliphatic rings connected by flexile moieties, 1D- and 2D-ordered

394   phases can develop, arising from Van der Waals forces, π-π stacking and polar interactions.[78-82]

395   Barrier properties also depend on the possibility of ring flipping,[83] and of macromolecular

396   arrangements, which may affect the overall dipolar moment without changing the chemistry.[84] In

397   addition to them, in the case of furan-based polymers, the establishment of hydrogen bonds can be

398   also considered.[32,33,71,72] PDEF gas barrier properties were analysed and compared with those of PBF

399   and PPeF.

400   The permeability performances to two different pure gases, O_2 and CO_2, were evaluated on the

401   compression moulded films. In **Fig. 5A** the results, expressed as gas transmission rate (GTR), were

402 reported. The experiments were conducted sequentially, as follows: i) temperature (T) 23°C, relative

403 humidity (RH) 0%; ii) T 23°C, RH 85%; iii) T 23°C, RH 0%. From the first test conducted at 23°C

404 in dry atmosphere, it was clear that PBF presented the highest values of GTR among the series, despite

405 its higher glass transition temperature and semicrystalline nature. Differently, PDEF and PPeF, even

406 though amorphous and with T_g values around the temperature of measuring, resulted very outstanding

407 and with comparable performance. An explanation could be found, as mentioned before, in the

408 presence of a particular macromolecular arrangement that blocked the passage of gases through the

409 materials.[85] In the case of PPeF, as previously reported,[32,33] 1-D, 2D-ordered domains developed

410 during compression moulding with consequent improvement of gas barrier performance. This

411 peculiar microstructure originated from inter-chain hydrogen bonds, these last also present, and to

412 greater extent, in PDEF. The presence of ether-oxygen atom in PDEF repeating unit enhanced the

413 number of hydrogen bonds favouring the inter-molecular forces. These last lead to a compact array,

414 that hampered the gas molecules passage. At the same time, the insertion of an oxygen atom into the

415 glycol subunit decreases the symmetry of the aliphatic segment, reducing the macromolecular sorting.

416 In other words, the density of the inter-chain hydrogen bond increases due to the presence of ether O

417 atoms, but their random distribution determines a not enough long chain arrangement, not detectable

418 through diffractometric measurements. Nevertheless, unexpectedly, the barrier performances of the

419 PDEF were not superior to those of PPeF. The result could be explained considering that the

420 formation of the compact array is somewhat contrasted by the lower mobility of the PDEF

421 macromolecular chains compared to those of the PPEF ($T_{g,PDEF} > T_{g,PPeF}$).

422 Afterwards, the three films were subjected to permeability tests at 85% RH, keeping the temperature

423 constant at 23°C. In case of PBF, an improvement of barrier performance was observed, while for

424 PDEF, permeability values remained almost constant. The result was quite surprising considering the

425 usually observed plasticizing effect of water, which, enhancing the chain mobility, determined an

426 increment of the free volume. On the other side, the same plasticizing effect detected for PPeF, caused

427 a slight increase of GTR values under humid conditions. To explain the behaviour of PDEF and PBF

428   films, it was supposed that water enhanced the inter-chain interactions occupying the empty sites at

429   the oxygen atoms of the furan ring and, in case of PDEF, also at the oxygen of the glycolic subunit.

430   Hence, a more compact and dense new structure was formed, responsible for the decreasing of the

431   GTR values.[85] In the case of PPeF, also containing furan O atoms in the furan ring, the longer glycolic

432   part compared to PBF decreased the density of furan ring per unit length. Therefore, the plasticizing

433   effect of water prevailed on the formation of a more compact microstructure arising from the

434   hydrogen bonds establishment. In PDEF, characterized by repeating unit length comparable to PPeF,

435   the presence of the oxygen atom instead of the central methylene group explained the different

436   behaviour in wet environment.

437   In the third experiment, the films were firstly subjected to vacuum in order to remove the moisture

438   residues and then, a new test was performed at 23°C and 0% RH. PBF and PDEF maintained the

439   same good performances reached under humid conditions. It is plausible that the vacuum applied was

440   not affecting the hydrogen bonds formed among water and furan/ether oxygen. For PPeF, it could be

441   hypothesized that the free molecules of water trapped inside the material and acting as plasticizer,

442   were removed by vacuum. Conversely, those forming hydrogen bonds with the furan ring remained

443   inside the material, making GTR-O_2 value decrease and GTR-CO_2 one almost unvaried.

444   Another aspect to consider was the different perm-selectivity ratio, defined as GTR_{CO_2}/GTR_{O_2}, which

445   is an indication of the different barrier performance towards the two gases. It should be remembered

446   that oxygen is a small and no-polar molecule characterized by a transmission rate lower than that of

447   the larger carbon dioxide, which contains polar C-O covalent bonds.[50] Consequently, the perm-

448   selectivity ratio is usually higher than 1. Usually, in polyesters $GTR_{CO_2} > GTR_{O_2}$, meaning carbon

449   dioxide passed through the films easier than O_2. In the furan-based polyesters, a peculiar behaviour

450   with particularly low GTR values for CO_2 had been documented.[32,86-88] This evidence was ascribed

451   to the presence of permanent dipoles in CO_2 interacting with the polar groups of polymeric chains

452 (furan ring), thus increasing CO_2 solubility and simultaneously decreasing its diffusivity. The

453 consequent result is a GTR_{CO_2}/GTR_{O_2} ratio close to 1 for furan-containing polyesters.

454

455
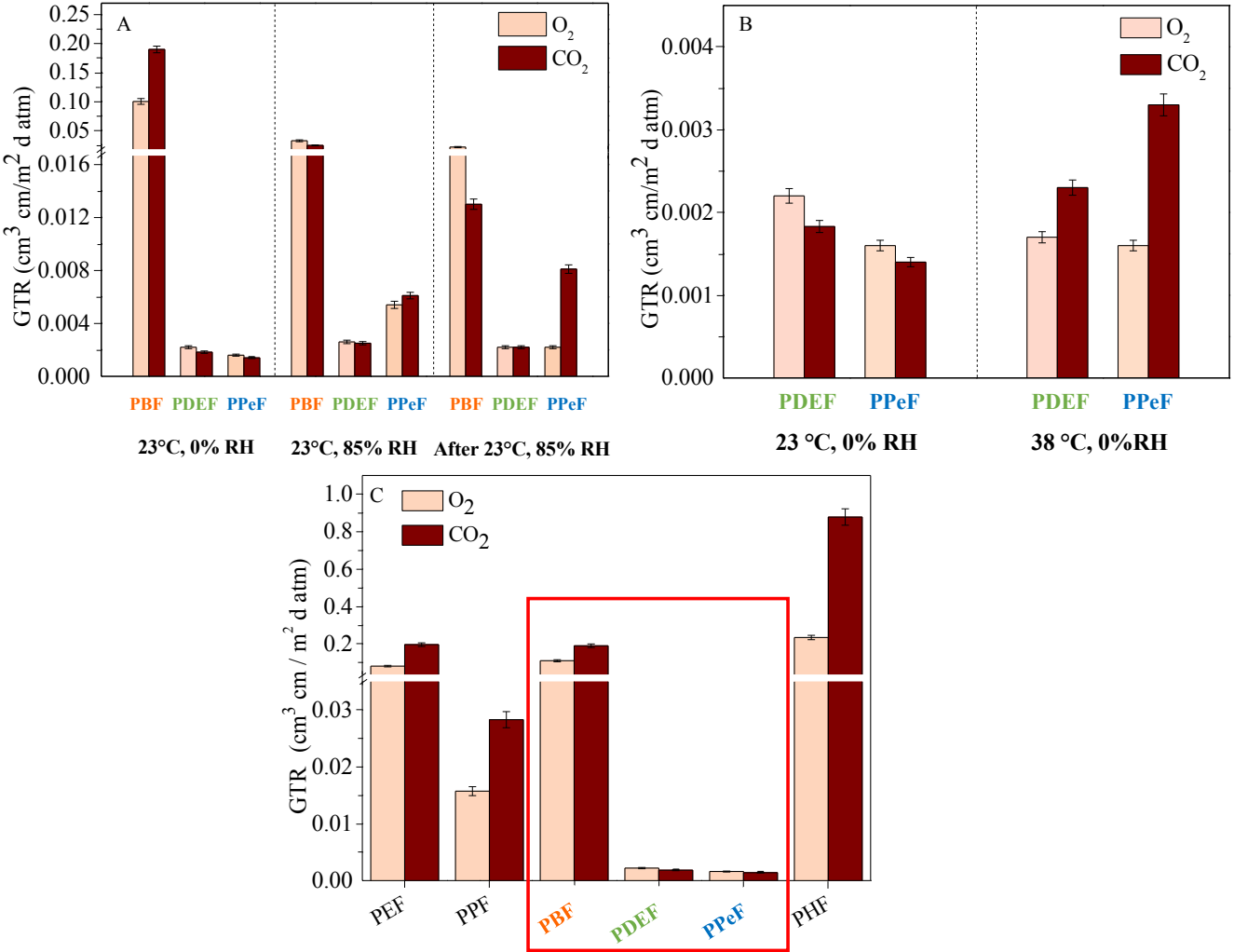
456 **Fig. 5. A)** GTR-O_2 and -CO_2 of PBF, PDEF and PPeF, for three subsequent experiments conducted

457 at 23°C in different conditions of humidity; **B)** GTR-O_2 and -CO_2 of PDEF and PPeF at 23 and 38

458 °C; **C)** GTR-O_2 and -CO_2 of different furan-based polyesters (PEF[34], PPF[10], PHF[10]).

459

460

461 Considering the three-step experiment reported in **Fig. 5A**, a different effect of humidity conditions

462 on perm-selectivity ratio could be found for PBF, PDEF and PPeF films.

463   As concerns PBF, in the first test conducted, the driving force was the dimension of the molecules.

464   Operating at 85% RH, new polar interactions between water molecules and polymer chains formed,

465   favouring CO_2 solubility. The effect kept constant even returning to dry environment.

466   In case of PDEF, its higher polarity due to the O atom insertion in the PBF backbone, helped to

467   maintain the GTR_{CO_2}/GTR_{O_2} ratio always close to 1. As regards PPeF, the trend observed was

468   different: humidity determined an increment of perm-selectivity ratio, which further increased after

469   removing free water molecules by vacuum. This trend could be explained considering that H_2O first

470   acted as plasticizer, enhancing polymer chain mobility, and then left vacancies after vacuum was

471   applied. Both these effects increased the free volume, favouring mainly the passage of the fastest CO_2

472   molecules. These last, in turn, were less soluble in PPeF than in PBF and especially in PDEF films.

473   PDEF and PPeF were also tested at 38°C to simulate hot weather conditions. As one can see from

474   **Fig. 5B**, despite at this temperature macromolecular chains of both polymers were in a complete

475   mobile state, barrier properties did not suffer a general worsening. This experiment supports, one

476   more time, the hypothesis of supramolecular arrays originated from hydrogen bonds among the

477   chains. As evident, these compact structures were not affected by the increasing of temperature, since

478   the polymers maintain their performances. Differently, the increase of temperature in case of common

479   polyesters leads to higher free volume among the macromolecules, favouring gas permeation.

480   Anyway, an increase of CO_2 gas transmission rate was detected by increasing temperature. As already

481   mentioned, the gas passage depended on both solubility and diffusivity. This latter generally rises

482   with temperature, the effect being more intense for the gas molecules characterized by the most

483   chaotic motions, such as CO_2 molecules. In both cases, the performances to O_2 at 23°C and 38°C

484   were constant, while GTR_{CO_2} values increased.

485   In **Fig. 5C**, a comparison of PDEF with PBF, PPeF and other furan-based polyesters was reported.

486   As one can see, PDEF and PPeF had GTR values much lower than the other materials.

487   In addition, an odd/even effect could be observed: the materials with odd number of -CH$_2$- groups

488   resulted more performant compared to the even numbered -CH$_2$- containing ones. Surprisingly, PDEF

489   and PPeF presented GTR values lower than those of PPF, despite their lower T$_g$ (T$_{g,PPeF}$ = 13°C;

490   T$_{g,PDEF}$ = 24°C; T$_{g,PPF}$ = 52°C). As previously reported, the deviating behaviour of PPeF and PDEF

491   could be attributed to the supramolecular compact phase coming from the hydrogen bond formation,

492   this last being favoured in rubbery amorphous furan-polyesters as PDEF and PPeF.

493   As regards the materials containing an even number of -CH$_2$- groups, PEF, PBF and PHF, a

494   progressive worsening of gas barrier performances can be observed, ascribable to different reasons

495   as previously reported:[33,89] (i) increasing amount of the so called disclinations; (ii) increasing fraction

496   of 3D-ordered phase at the expense of the more performant 2D-one; (iii) increasing of free volume

497   fraction (T$_{g,PEF}$>T$_{g,PBF}$ >T$_{g,PHF}$).

498   **4. Conclusions**

499   The use of traditional synthetic Ti-based catalysts together with an optimized solvent-free two-stage

500   polycondensation process permitted to obtain a 100% bio-based high molecular weight

501   poly(diethylene 2,5-furanoate) (PDEF). The polymer could be processed in form of thin freestanding

502   films by compression moulding, although completely amorphous and with a T$_g$ around room

503   temperature. A similar behaviour was previously observed for poly(pentamethylene 2,5-furanoate)

504   (PPeF), with respect to which the polymer object of this study has some important similarities in

505   terms of properties. In particular, both polyesters are characterized by very high thermal stability

506   (PDEF's one even slightly higher than that of PPeF), exceptional gas barrier properties both at room

507   temperature and at 38°C, preserved in the presence of humidity. Lastly, they are both compostable,

508   although PDEF degrades much faster than PPeF, mainly due to its greater hydrophilicity. In terms of

509   mechanical response, a fundamental property for a possible application in food packaging, PDEF

510   showed an intermediate behaviour between poly(butylene 2,5-furanoate) (PBF) and PPeF. In fact,

511   PDEF film exhibited the flexibility typical of PPeF, even though not an elastomeric behaviour (PDEF

24

512 stress-strain curve shows yielding), but a much higher elastic modulus and stress at break as PBF,

513 which confer to the material toughness and ductility. Therefore, with PDEF both the mechanical

514 limits of PBF (brittleness) and of PPeF (too high softness) are overcome, without compromising the

515 outstanding thermal stability, gas barrier properties and compostability of PPeF. The goal was

516 achieved through a small chemical modification of polymer chemical structure, i.e. the insertion of

517 an ether oxygen atom into the glycol subunit, centrally positioned. As known from basic chemistry,

518 oxygen is characterized by high electronegativity and small dimensions, and these characteristics

519 have had a significant impact on the final properties of the polymer. Specifically:

520 - The lower dimension of oxygen with respect to carbon atom affected the chain constitutional

521 regularity with consequent suppression of the polymer crystallization capacity (PDEF is

522 amorphous, whereas PBF is semicrystalline). Moreover, C-O bond is shorter than C-C one,

523 implying for ethereal bond a higher energy (PDEF is more thermally stable than PBF); the

524 insertion of an oxygen atom in glycol subunit also makes its polymer chain more flexible than

525 that of PBF, the aliphatic part being longer;

526 - The high oxygen electronegativity strengthens inter-chain interactions (hydrogen bonds

527 involving furan ring and Van der Waals interactions) responsible of the outstanding gas

528 barrier (similar to those of PPeF) and mechanical properties (better than those of both PBF

529 and PPeF) and increases polymer hydrophilicity, the parameter determining the very fast

530 compostability of this polyester.

531 In conclusion, PDEF represents a very promising candidate to obtain an easily recyclable mono-

532 material package and also for producing single-use plastic packaging compostable in just one day.

533

534 **Author contributions**

535   S.Q. M.S. synthesized and characterized the polymer. V.S. performed gas barrier measurements.

536   S.Q., G.G., M.S. and N.L. analyzed the overall experimental data. M.S. and N.L. wrote manuscript.

537   G.G., M.S. and N. L. corrected and reviewed the manuscript. N.L. supervised and financed the work.

Conflicts of interest

539   The authors declare no conflict of interests.

Acknowledgments

Supplementary data

546   These files can be found in the supplementary data:

547   Fig. S1. ^{1}H-NMR spectra of PBF, PDEF and PPeF (from the top to the bottom) with the relative peak

548   assignment.

549

References

551   1. Plastics   -   The   facts   2020.   *PlasticsEurope,*   2020,

552   https://www.plasticseurope.org/en/resources/publications/4312-plastics-facts-2020 (accessed

553   July 2021).

554   2. https://www.statista.com/statistics/664906/plastics-production-volume-forecast-worldwide/

555   STATISTA 2021 (accessed September 2021).

556   3. Plastic Market Size, Share & Trends Analysis Report by Product (PE, PP, PU, PVC, PET,

557   Polystyrene, ABS, PBT, PPO, Epoxy Polymers, LCP, PC, Polyamide), by Application, by

End-use, by Region, and Segment Forecasts, 2021 – 2028, Grand view Research 2021 (accessed: September 2021).

4. RameshKumar, S.; Shaiju, P.; O'Connor, K. E.; P, R. B. Bio-Based and Biodegradable Polymers - State-of-the-Art, Challenges and Emerging Trends. *Curr. Opin. Green Sustain. Chem*. **2020**, *21*, 75–81.

5. Mülhaupt, R. Green Polymer Chemistry and Bio-based Plastics: Dreams and Reality. *Macromol. Chem. Phys*. **2013**, *214*, 159–174.

6. Rabnawaz, M.; Wyman, I.; Auras, R.; Cheng, S. A roadmap towards green packaging: the current status and future outlook for polyesters in the packaging industry. *Green Chem*. **2017**, *19*, 4737-4753.

7. Álvarez-Chávez, C. R.; Edwards, S.; Moure-Eraso, R; Geiser, K. Sustainability of bio-based plastics: General comparative analysis and recommendations for improvement. *J. Clean Prod*. **2012**, *23*, 47–56.

8. Papageorgiou, G. Z. Thinking Green: Sustainable Polymers from Renewable Resources. *Polymers* **2018**, *10*, 952.

9. Zhang, Q.; Song, M.; Xu, Y.; Wang, W.; Wang, Z.; Zhang, L. Bio-based polyesters: Recent progress and future prospects. *Prog. Polym. Sci*. **2021**, *120,* 101430.

10. Morris, A. B. *The Science and Technology of Flexible Packaging. Multilayer Films from Resin and Process to End Use,* Elsevier, **2016**.

11. Reichert, C. L.; Bugnicourt, E.; Coltelli, M.-B.; Cinelli, P.; Lazzeri, A.; Canesi, I.; Braca, F.; Martínez, B. M.; Alonso, R.; Agostinis, L.; Verstichel, S.; Six, L.; De Mets, S.; Gómez, E. C.; Ißbrücker, C.; Geerinck, R.; Nettleton, D. F.; Campos, I.; Sauter, E.; Pieczyk, P.; Schmid, M. Bio-Based Packaging: Materials, Modifications, Industrial Applications and Sustainability. *Polymers* **2020**, *12*, 1558.

12. Young, E.; Mirosa, M.; Bremer, P. A Systematic Review of Consumer Perceptions of Smart Packaging Technologies for Food. *Front. Sustain. Food Syst*. **2020**, *4*, 63.

584   13. Majid, I.; Nayik, G. A.; Dar, S. M.; Nanda, V. Novel food packaging technologies:

585   Innovations and future prospective. *J. Saudi Soc. Agric. Sci.* **2018**, *17*, 454-462.

586   14. Bhargava, N.; Sharanagat, V. S.; S Mor, R.; Kumar, K. Active and intelligent biodegradable

587   packaging films using food and food waste-derived bioactive compounds: A review. *Trends*

588   *Food Sci. Technol.* **2020**, *105*, 385-401.

589   15. Firouz, M. S.; Mohi-Alden, K.; Omid, M. A critical review on intelligent and active packaging

590   in the food industry: Research and development. *Food Res. Int.* **2021**, *141*, 110113.

591   16. Singh, G.; Singh, S.; Kumar, B.; Gaikwad, K. K. Active barrier chitosan films containing

592   gallic acid based oxygen scavenger. *J. Food Meas. Charact.* **2021**, *15*, 585–593.

593   17. https://perfectpackaging.org (accessed: September 2021).

594   18. https://www.flexpack-europe.org (accessed: September 2021).

595   19. Vilela, C.; Sousa, A. F.; Fonseca, A. C.; Serra, A. C.; Coelho, J. F. J.; Freire, C. S. R.;

596   Silvestre, A. J. D. The quest for sustainable polyesters – insights into the future. *Polym. Chem.*

597   **2014**, *5*, 3119-3141.

598   20. Hwang, K. R.; Jeon, W.; Lee, S. Y.; Kim, M. S.; Park, Y. K. Sustainable bioplastics: Recent

599   progress in the production of bio-building blocks for the bio-based next-generation polymer

600   PEF. *Chem. Eng. J.* **2020**, *390*, 124636.

601   21. Sousa, A. F.; Vilela, C.; Fonseca, A. C.; Matos, M.; Freire, C. S. R.; Gruter, G. J. M.; Coelho,

602   J. F. J.; Silvestre, A. J. D. Biobased polyesters and other polymers from 2,5-furandicarboxylic

603   acid: a tribute to furan excellency. *Polym. Chem.* **2015**, *6*, 5961-5983.

604   22. Papageorgiou, G. Z.; Papageorgiou, D. G.; Terzopoulou, Z.; Bikiaris, D. N. Production of bio-

605   based 2,5-furan dicarboxylate polyesters: Recent progress and critical aspects in their

606   synthesis and thermal properties. *Eur. Polym. J.* **2016**, *83*, 202-229.

607   23. Loos, K.; Zhang, R.; Pereira, I.; Agostinho, B.; Hu, H.; Maniar, D.; Sbirrazzuoli, N.; Silvestre,

608   A. J. D.; Guigo, N.; Sousa, A. F. A Perspective on PEF Synthesis, Properties, and End-Life.

609   *Front. Chem.* **2020**, *8*, 585.

28

610   24. Terzopoulou, Z.; Papadopoulos, L.; Zamboulis, A.; Papageorgiou, D. G.; Papageorgiou, G.

611   Z.; Bikiaris, D. N. Tuning the Properties of Furandicarboxylic Acid-Based Polyesters with

612   Copolymerization: A Review. *Polymers* **2020**, *12*, 1209.

613   25. Iglesias, J.; Martínez-Salazar, I.; Maireles-Torres, P.; Martin Alonso, D.; Mariscal, R; López

614   Granados, M. Advances in catalytic routes for the production of carboxylic acids from

615   biomass: a step forward for sustainable polymers. *Chem. Soc. Rev*. **2020**, *49*, 5704-5771.

616   26. Chen, C.; Wang, L.; Zhu, B.; Zhou, Z.; El-Hout, S. I.; Yang, J.; Zhang, J. 2,5-

617   Furandicarboxylic acid production via catalytic oxidation of 5-hydroxymethylfurfural:

618   Catalysts, processes and reaction mechanism. *J. Energy Chem*. **2021**, *54*, 528-554.

619   27. Wojcieszak, R.; Itabaiana, I. Engineering the future: Perspectives in the 2,5-furandicarboxylic

620   acid synthesis. *Catal. Today* **2020**, *354*, 211-217.

621   28. Dedes, G.; Karnaouri, A.; Topakas, E. Novel Routes in Transformation of Lignocellulosic

622   Biomass to Furan Platform Chemicals: From Pretreatment to Enzyme Catalysis. *Catalysts*

623   **2020**, *10*, 743.

624   29. Wu, S.; Liu, Q.; Tan, H.; Zhang, F.; Yin, H. A Novel 2,5-Furandicarboxylic Acid Biosynthesis

625   Route from Biomass-Derived 5-Hydroxymethylfurfural Based on the Consecutive Enzyme

626   Reactions. *Appl. Biochem. Biotechnol*. **2020**, *191*, 1470–1482.

627   30. Naim, W.; Schade, O. R.; Saraci, E.; Wust, D.; Kruse, A.; Grundwaldt, J. D. Toward an

628   Intensified Process of Biomass-Derived Monomers: The Influence of 5-

629   (Hydroxymethyl)furfural Byproducts on the Gold-Catalyzed Synthesis of 2,5-

630   Furandicarboxylic Acid. *ACS Sustainable Chem. Eng*. **2020**, *8*, 11512–11521.

631   31. Deshan, A. D. K.; Atanda, L.; Moghaddam, L.; Rackemann, D. W.; Beltramini, J.; Doherty,

632   W. O. S. Heterogeneous Catalytic Conversion of Sugars Into 2,5-Furandicarboxylic Acid.

633   *Front. Chem*. **2020**, *8*, 659.

634   32. Guidotti, G.; Soccio, M.; García-Gutiérrez, M. C.; Gutiérrez-Fernández, E.; Ezquerra, T. A.;

635   Siracusa, V.; Munari, A.; Lotti, N. Evidence of a 2D-Ordered Structure in Biobased

Poly(pentamethylene furanoate) Responsible for Its Outstanding Barrier and Mechanical Properties. *ACS Sustainable Chem. Eng*. **2019**, *7*, 17863−17871.

33. Guidotti, G.; Soccio, M.; García-Gutiérrez, M. C.; Ezquerra, T.; Siracusa, V.; Gutiérrez-Fernández, E.; Munari, A.; Lotti, N. Fully Biobased Superpolymers of 2,5-Furandicarboxylic Acid with Different Functional Properties: From Rigid to Flexible, High Performant Packaging Materials. *ACS Sustainable Chem. Eng.* **2020**, *8*, 9558–9568.

34. Benson, N. U.; Bassey D. E.; Palanisami, T. COVID pollution: impact of COVID-19 pandemic on global plastic waste footprint. *Heliyon* **2021**, *7*, e06343.

35. Klemeš, J. J.; Van Fan, Y.; Tan, R. R.; Jiang, P. Minimising the present and future plastic waste, energy and environmental footprints related to COVID-19. *Renewable Sustainable Energy Rev*. **2020**, *127*, 109883.

36. Khoo, K. S.; Ho, L. Y.; Lim, H. R.; Leong, H. Y.; Chew, K. W. Plastic waste associated with the COVID-19 pandemic: Crisis or opportunity? *J. Hazard. Mater*. **2021**, *417*, 126108.

37. Pellis, A.; Haernvall, K.; Pichler, C. M.; Ghazaryan, G.; Breinbauer, R.; Guebitz, G. M. Enzymatic hydrolysis of poly(ethylene furanoate). *J. Biotechnol.* **2016**, *235*, 47-53.

38. Gigli, M.; Quartinello, F.; Soccio, M.; Pellis, A.; Lotti, N.; Guebitz, G. M.; Licoccia, S.; Munari, A. Enzymatic hydrolysis of poly(1,4-butylene 2,5-thiophenedicarboxylate) (PBTF) and poly(1,4-butylene 2,5-furandicarboxylate) (PBF) films: A comparison of mechanisms. *Environ. Int*. **2019**, *130*, 104852.

39. Okada, M.; Tachikawa, K.; Aoi, K. Biodegradable polymers based on renewable resources. II. Synthesis and biodegradability of polyesters containing furan rings. *J. Polym. Sci., Part A: Polym. Chem*. **1997**, *35*, 2729−2737.

40. Muller, R. J.; Kleeberg, I.; Deckwer, W. D. Biodegradation of polyesters containing aromatic constituents. *J. Biotechnol*. **2001**, *86*, 87–95.

660   41. Soccio, M.; Costa, M.; Lotti, N.; Gazzano, M.; Siracusa, V.; Salatelli, E.; Manaresi, P.;

661   Munari, A. Novel fully biobased poly(butylene 2,5-furanoate/diglycolate) copolymers

662   containing ether linkages: Structure-property relationships. *Eur. Polym. J.* **2016**, *81*, 397–412.

663   42. Guidotti, G.; Soccio, M.; Lotti, N.; Siracusa, V.; Gazzano, M.; Munari, A. New multi-block

664   copolyester of 2,5-furandicarboxylic acid containing PEG-like sequences to form flexible and

665   degradable films for sustainable packaging. *Polym. Degrad. Stab.* **2019**, *169*, 108963.

666   43. Cowie, J. M. G.; Arrighi, V. *Polymers Chemistry and Physics of Modern Materials*, 3rd

667   Edition, CRC Press, **2007**, Chapter 15.

668   44. Poulopoulou, N.; Smyrnioti, D.; Nikolaidis, G. N.; Tsitsimaka, I.; Christodoulou, E.; Bikiaris,

669   D. N.; Charitopoulou, M. A.; Achilias, D. S.; Kapnisti, M.; Papageorgiou, G. Z. Sustainable

670   Plastics from Biomass: Blends of Polyesters Based on 2,5-Furandicarboxylic Acid. *Polymers*

671   **2020**, *12*, 225.

672   45. Thiyagarajan, S.; Vogelzang, W.; Knoop, R. J. I.; Frissen, A. E.; van Haveren, J.; van Es, D.

673   S. Biobased furandicarboxylic acids (FDCAs): effects of isomeric substitution on polyester

674   synthesis and properties. *Green Chem.* **2014**, *16*, 1957-1966.

675   46. Soccio, M.; Nogales, A.; García-Gutiérrez, M.; Lotti, N.; Munari, A.; Ezquerra, T. Origin of

676   the subglass dynamics in aromatic polyesters by labeling the dielectric relaxation with ethero

677   atoms. *Macromolecules* **2008**, *41*, 2651–2655.

678   47. Bianchi, E.; Soccio, M.; Siracusa, V.; Gazzano, M.; Thiyagarajan, S.; Lotti, N. Poly(butylene

679   2,4-furanoate), an Added Member to the Class of Smart Furan-Based Polyesters for

680   Sustainable Packaging: Structural Isomerism as a Key to Tune the Final Properties. *ACS*

681   *Sustainable Chem. Eng.* **2021**, *9*, 11937–11949.

682   48. Thiyagarajan, S.; Meijlink, M. A.; Bourdet, A.; Vogelzang, W.; Knoop, R. J. I.; Esposito, A.;

683   Dargent, E.; van Es, D. S.; van Haveren, J. Synthesis and Thermal Properties of Bio-Based

684   Copolyesters from the Mixtures of 2,5- and 2,4-Furandicarboxylic Acid with Different Diols.

685   *ACS Sustainable Chem. Eng.* **2019**, *7*, 18505–18516.

686   49. Nolasco, M. M.; Araujo, C. F.; Thiyagarajan, S.; Rudić, S.; Vaz, P. D.; Silvestre, A. J. D.;

687   Ribeiro-Claro, P. J. A.; Sousa, A. F. Asymmetric Monomer, Amorphous Polymer? Structure–

688   Property Relationships in 2,4-FDCA and 2,4-PEF. *Macromolecules* **2020**, *53*, 1380–1387.

689   50. Robertson, G. L. *Food Packaging Principles and Practice*, 3rd Edition, CRC Press, **2013**,

690   Chapter 2-4.

691   51. Davidson, M. G.; Elgie, S.; Parsons, S.; Young, T. J. Production of HMF, FDCA and their

692   derived products: a review of life cycle assessment (LCA) and techno-economic analysis

693   (TEA) studies. *Green Chem.* **2021**, *23*, 3154-3171.

694   52. Bozell, J. J.; Petersen, G. R. Technology development for the production of biobased products

695   from biorefinery carbohydrates—the US Department of Energy's "Top 10" revisited. *Green*

696   *Chem.* **2010**, *12*, 539-554.

697   53. Bio-Based Chemicals A 2020 Update, IEA Bioenergy, available online:

698   https://www.ieabioenergy.com/wp-content/uploads/2020/02/Bio-based-chemicals-a-2020-

699   update-final-200213.pdf (accessed September 2021).

700   54. Zheng, M.; Li, X. Y.; Guan, R. Q.; Liu, Y. M.; Zhao, Y. J.; Tai, Y. L. Ionic Liquid-Catalyzed

701   Synthesis of Diethylene Glycol. *Adv. Mat. Res.* **2012**, *549*, 287-291.

702   55. Bioplastics market data, European-bioplastics.org (accessed September 2021).

703   56. Soccio, M.; Lotti, N.; Finelli, L.; Gazzano, M.; Munari, A. Influence of transesterification

704   reactions on the miscibility and thermal properties of poly(butylene/diethylene succinate)

705   copolymers. *Eur. Polym. J.* **2008**, *44*, 1722-1732.

706   57. Soccio, M.; Lotti, N.; Gigli, M.; Finelli, L.; Gazzano, M.; Munari, A. Reactive blending of

707   poly(butylene succinate) and poly(triethylene succinate): characterization of the copolymers

708   obtained. *Polym. Int.* **2012**, *61*, 1163-1169.

709   58. Fabbri, M.; Gigli, M.; Gamberini, R.; Lotti, N.; Gazzano, M.; Rimini, B.; Munari, A.

710   Hydrolysable PBS-based poly(ester urethane)s thermoplastic elastomers. *Polym. Degrad.*

711   *Stab.* **2014**, *108*, 223-231.

712 59. Lotti, N.; Finelli, L.; Fiorini, M.; Righetti, M. C.; Munari, A. Synthesis and characterization

713 of poly(butylene terephthalate-co-diethylene terephthalate) copolyesters. *Polymer* **2000**, 41,

714 5297-5304.

715 60. Lotti, N.; Finelli, L.; Fiorini, M.; Righetti, M. C.; Munari, A. Synthesis and characterization

716 of poly(butylene terephthalate-co-triethylene terephthalate) copolyesters. *J. Appl. Polym. Sci.*

717 **2001**, *81*, 981-990.

718 61. Gigli, M.; Lotti, N.; Gazzano, M.; Finelli, L.; Munari, A. Novel eco-friendly random

719 copolyesters of poly(butylene succinate) containing ether-linkages. *React. Funct. Polym.*

720 **2012**, *72*, 303-310.

721 62. Gigli, M.; Lotti, N.; Gazzano, M.; Siracusa, V.; Finelli, L.; Munari, A.; Dalla Rosa, M. Fully

722 aliphatic copolyesters based on poly(butylene 1,4-cyclohexanedicarboxylate) with promising

723 mechanical and barrier properties for food packaging applications. *Ind. Eng. Chem. Res.* **2013**,

724 *52*, 12876−12886.

725 63. Gigli, M.; Lotti, N.; Gazzano, M.; Siracusa, V.; Finelli, L.; Munari, A.; Dalla Rosa, M.

726 Biodegradable aliphatic copolyesters containing PEG-like sequences for sustainable food

727 packaging applications. *Polym. Degrad. Stab.* **2014**, *105*, 96-106.

728 64. Kainulainen, T. P.; Hukka, T. I.; Ozeren, H. D.; Sirvio, J. A.; Hedenqvist, M. S.; Heiskanen,

729 J. P. Utilizing Furfural-Based Bifuran Diester as Monomer and Comonomer for High-

730 Performance Bioplastics: Properties of Poly(butylene furanoate), Poly(butylene bifuranoate),

731 and Their Copolyesters. *Biomacromolecules* **2020**, *21*, 743−752.

732 65. Jiang, Y.; Woortman, A. J. J.; Alberda van Ekensteina, G. O. R.; Loos, K. A biocatalytic

733 approach towards sustainable furanic–aliphatic polyesters. *Polym. Chem.* **2015**, *6*, 5198-5211.

734 66. Haernvall, K.; Zitzenbacher, S.; Amer, H.; Zumstein, M. T.; Sander, M.; McNeill, K.;

735 Yamamoto, M.; Schick, M. B.; Ribitsch, D.; Guebitz, G. M. Polyol Structure Influences

736 Enzymatic Hydrolysis of Bio-Based 2,5-Furandicarboxylic Acid (FDCA) Polyesters.

737 *Biotechnol. J.* **2017**, *12*, 1600741.

33

67. Papageorgiou, G. Z.; Papageorgiou, D. G.; Terzopoulou, Z.; Bikiaris, D. N. Production of bio-based 2,5-furan dicarboxylate polyesters: Recent progress and critical aspects in their synthesis and thermal properties. *Eur. Polym. J*. **2016**, *83*, 202-229.

68. Tsanaktsis, V.; Terzopoulou, Z.; Nerantzaki, M.; Papageorgiou, G. Z.; Bikiaris, D. N. New poly(pentylene furanoate) and poly(heptylene furanoate) sustainable polyesters from diols with odd methylene groups. *Mater. Lett*. **2016**, *178*, 64-67.

69. Diao, L.; Su, K.; Li, Z.; Ding, C. Furan-based co-polyesters with enhanced thermal properties: poly(1,4-butylene-co-1,4-cyclohexanedimethylene-2,5-furandicarboxylic acid) *RSC Adv.* **2016**, *6*, 27632-27639.

70. Cottrell, T. L. *The Strengths of Chemical Bonds*, Butterworths, 2nd ed., London, 1958.

71. Martinez-Tong, D. E.; Soccio, M.; Robles-Hernández, B.; Guidotti, G.; Gazzano, M.; Lotti, N.; Alegria, A. Evidence of Nanostructure Development from the Molecular Dynamics of Poly(pentamethylene 2,5-furanoate). *Macromolecules* **2020**, *53*, 10526-10537.

72. Araujo, C. F.; Nolasco, M. M.; Ribeiro-Claro, P. J. A.; Rudic, S.; Silvestre, A. J. D.; Vaz, P. D.; Sousa, A. F. Inside PEF: chain conformation and dynamics in crystalline and amorphous domains. *Macromolecules* **2018**, *51*, 3515–3526.

73. Patkar, M.; Jabarin, S. A. Effect of diethylene glycol (DEG) on the crystallization behavior of poly(ethylene terephthalate) (PET). *J. Appl. Polym. Sci*. **1993**, *47*, 1749-1763.

74. Soccio, M.; Lotti, N.; Finelli, L.; Gazzano, M.; Munari, A. Aliphatic poly(propylene dicarboxylate)s: Effect of chain length on thermal properties and crystallization kinetics. *Polymer* **2007**, *48*, 3125-3136.

75. Liang, H.; Hao, Y.; Liu, S.; Zhang, H.; Li, Y.; Dong, L.; Zhang, H. Thermal, rheological, and mechanical properties of polylactide/poly(diethylene glycol adipate). *Polym. Bull*. **2013**, *70*, 3487–3500.

76. Cao, A.; Okamura, T.; Nakayama, K.; Inoue, Y.; Masuda, T. Studies on syntheses and physical properties of biodegradable aliphatic poly(butylene succinate-co-ethylene

764 succinate)s and poly(butylene succinate-co-diethylene glycol succinate)s. *Polym. Degrad.*

765 *Stab*. **2002**, *78*, 107-117.

766 77. Zeng, J. B.; Huang, C. L.; Jiao, L.; Lu, X.; Wang, Y. Z.; Wang, X. L. Synthesis and Properties

767 of Biodegradable Poly(butylene succinate-co-diethylene glycol succinate) Copolymers. *Ind.*

768 *Eng. Chem. Res*. **2012**, *51*, 12258–12265.

769 78. Rudyak, V. Y.; Gavrilov, A. A.; Guseva, D. V.; Tung, S. H.; Komarov, P. V. Accounting for

770 π–π stacking interactions in the mesoscopic models of conjugated polymers. *Mol. Syst. Des.*

771 *Eng*. **2020**, *5*, 1137.

772 79. Sago, T.; Itagaki, H.; Asano, T. Onset of Forming Ordering in Uniaxially Stretched

773 Poly(ethylene terephthalate) Films Due to π−π Interaction Clarified by the Fluorescence.

774 *Macromolecules* **2014**, *47*, 217−226.

775 80. Shanavas, A.; Sathiyaraj, S.; Chandramohan, A.; Narasimhaswamy, T.; Sultan Nasar, A.

776 Isophthalic acid based mesogenic dimers: Synthesis and structural effects on mesophase

777 properties. *J. Mol. Struct*. **2013**, *1038*, 126-133.

778 81. Mahendrasingam, A.; Blundell, D. J.; Martin, C.; Urban, V.; Narayanan, T.; Fuller, W. Time

779 resolved WAXS study of the role of mesophase in oriented crystallisation of poly(ethylene

780 terephthalate-co-isophthalate) copolymers. *Polymer* **2005**, *46*, 6044-6049.

781 82. Nolasco, M. M.; Araujo, C. F.; Thiyagarajan, S.; Rudić, S.; Vaz, P. D.; Silvestre, A. J. D.;

782 Ribeiro-Claro, P. J. A.; Sousa, A. F. Asymmetric Monomer, Amorphous Polymer? Structure–

783 Property Relationships in 2,4-FDCA and 2,4-PEF. *Macromolecules* **2020**, *53*, 1380−1387.

784 83. (Burgess, S. K.; Leisen J. E.; Kraftschik, B. E.; Mubarak, C. R., Kriegel, R. M.; Koros, W. J.

785 Chain Mobility, Thermal, and Mechanical Properties of Poly(ethylene furanoate) Compared

786 to Poly(ethylene terephthalate). *Macromolecules* **2014**, *47*, 1383−1391.

787 84. Bourdet, A.; Esposito, A.; Thiyagarajan, S.; Delbreilh, L.; Affouard, F.; Knoop, R. J. I.;

788 Dargent, E. Molecular Mobility in Amorphous Biobased Poly(ethylene 2,5-

789 furandicarboxylate) and Poly(ethylene 2,4-furandicarboxylate). *Macromolecules* **2018**, *51*,

790 1937−1945.

791 85. Hedenqvist, M. S. Barrier Packaging Materials, in: Kutz, M. (Ed.), *Handbook of*

792 *Environmental Degradation of Materials*, Elsevier Inc., 2nd ed., **2012**, pp. 833–860.

793 86. Burgess, S. K.; Kriegel, R. M.; Koros, W. J. Carbon dioxide sorption and transport in

794 amorphous poly (ethylene furanoate). *Macromolecules* **2015**, *48*, 2184–2193.

795 87. Guidotti, G.; Genovese, L.; Soccio, M.; Gigli, M.; Munari, A.; Siracusa, V.; Lotti, N. Block

796 Copolyesters Containing 2,5-Furan and trans-1,4-Cyclohexane Subunits with Outstanding

797 Gas Barrier Properties. *Int. J. Mol. Sci.* **2019**, *20*, 1–15.

798 88. Guidotti, G.; Soccio, M.; Lotti, N.; Gazzano, M.; Siracusa, V.; Munari, A. Poly (propylene 2,

799 5-thiophenedicarboxylate) vs. Poly (propylene 2, 5-furandicarboxylate): Two examples of

800 high gas barrier bio-based polyesters. *Polymers* **2018**, *10*, 785.

801 89. Guidotti, G.; Gigli, M.; Soccio, M.; Lotti, N.; Gazzano, M.; Siracusa, V.; Munari, A. Ordered

802 structures of poly (butylene 2, 5-thiophenedicarboxylate) and their impact on material

803 functional properties. *Eur. Polym. J.* **2018**, *106*, 284–290.